frontiers | Frontiers in Earth Science

ORIGINAL RESEARCH
published: 17 June 2022
doi: 10.3389/feart.2022.885197

Genetic Mechanism of Geothermal Anomaly in the Gaoyang Uplift of the Jizhong Depression

Qingzhuang Miao[1,2,3], Guiling Wang[2,3], Shihua Qi[1], Linxiao Xing[2,3], Hailiang Xin[4] and Xiaoni Zhou[2]*

[1]State Key Laboratory of Biogeology and Environmental Geology, School of Earth Sciences and Resources, China University of Geosciences, Wuhan, China, [2]Institute of Hydrogeology and Environmental Geology, Chinese Academy of Geological Sciences, Shijiazhuang, China, [3]Technology Innovation Center of Geothermal and Hot Dry Rock Exploration and Development, Ministry of National Resources, Shijiazhuang, China, [4]Geophysical Exploration Center, China Earthquake Administration, Zhengzhou, China

The Gaoyang uplift is rich in geothermal resources, but there are few studies on the regional geothermal genetic mechanism. A large number of geothermal wells fail in position calculation because of a shortage of basis. By using the methods of P-wave velocity structure imaging and magnetotelluric sounding, it draws the following conclusions: 1) The crustal thickness in the Gaoyang uplift area is relatively thin, about 32 km; 2) The cutting depth of the Gaoyang East fault exceeds 28 km and has reached the bottom of the lower crust. It is a large tensile fault that provides a channel for mantle heat flow into the shallow crust; 3) The Gaoyang uplift and its surrounding depressions form a concave-convex base fluctuation mode, which is conducive to the accumulation of heat flow to the uplift; 4) The deep carbonate thermal reservoir in the Gaoyang uplift is overlaid with Cenozoic sand and mudstone strata, with a thickness of more than 3000 m and low thermal conductivity, which is conducive to the preservation of thermal storage heat. Therefore, the shortening of the heat conduction path caused by regional crustal thinning, convective heat conduction of large faults, concave-convex structure, and thick Cenozoic caprock are the reasons why the heat reservoir temperature in the Gaoyang uplift is higher than that around, which provides a theoretical basis for geothermal development and utilization.

Keywords: p-wave, magnetotelluric sounding, depression, heat convection, Gaoyang uplift

OPEN ACCESS

Edited by:
Biao Shu,
Central South University, China

Reviewed by:
Sayantan Ganguly,
Indian Institute of Technology Ropar, India
Kunal Singh,
Geological Survey of India, India

***Correspondence:**
Guiling Wang
ihegwangguiling@sina.com

Specialty section:
This article was submitted to Solid Earth Geophysics, a section of the journal Frontiers in Earth Science

Received: *27 February 2022*
Accepted: *09 May 2022*
Published: *17 June 2022*

Citation:
Miao Q, Wang G, Qi S, Xing L, Xin H and Zhou X (2022) Genetic Mechanism of Geothermal Anomaly in the Gaoyang Uplift of the Jizhong Depression. Front. Earth Sci. 10:885197. doi: 10.3389/feart.2022.885197

INTRODUCTION

With the transformation of energy, geothermal energy as a green energy source has been confirmed by its actual utilization in China (Wang et al., 2017a). Nowadays, the continuous development of traditional non-renewable energy is gradually drying up, but the geothermal resources in the crust are rich in China. The total amount of hydrothermal geothermal resources in China is equivalent to 1.25 trillion standard tons of coal (Wang et al., 2020a). Although it cannot be compared with traditional energy at present, its influence will gradually become important because of carbon peak and carbon neutral. Therefore, it is increasingly becoming the concern of the majority of geological work. The direct utilization of geothermal energy has many benefits. The utilization of geothermal energy as a new energy source has been put forward for many years, which is of great significance for alleviating air pollution in China (Wang et al., 2017b).

The genetic mechanism of the geothermal field remains to be studied. Many scholars have done a lot of research on the abnormally high temperatures in geothermal fields (Chapman and

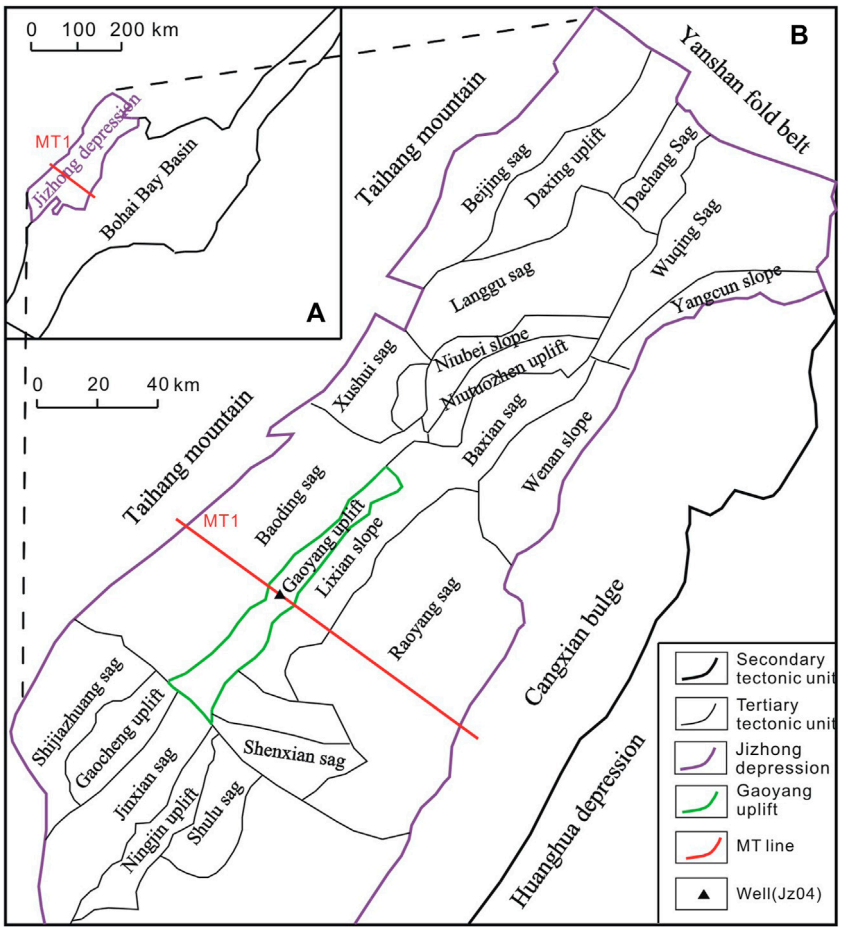

FIGURE 1 | (A) Location map of the Jizhong depression. **(B)** Schematic diagram of tectonic units in the Jizhong depression.

Rybach, 1985; Cermark and Rybach, 1989; Wang et al., 2001; Wang et al., 2017b; Lin et al., 2020). At present, it is generally believed that faults, radioactive heat generation, and mantle activity are the main causes of geothermal anomalies (Jaupart et al., 2015). Most scholars believe that the fault plays the role of a channel for thermal convection (Villas and Norton, 1977; Turcote and Schubert, 1982; Lin et al., 2020). High-temperature fluid in the deep can be obtained through the fault. Gao Z summarized the cause of abnormal geothermal temperatures according to practical experience, which is attributed to thermal convection with material exchange (Gao et al., 2009). Chen Moxiang and Deng Xiao believe that the underground heat flow in sedimentary basins always tends to have high thermal conductivity (Chen and Deng, 1990). It is suggested that the uplift zone has a high temperature, and the height of the geothermal field has a positive correlation with basement fluctuation. Aside from the aforementioned factors, many scholars also put forward that magmatic activity is the main factor in the geothermal field and believe that magmatic activity provides a steady stream of heat for the geothermal field (Urzua et al., 2002; Oskooi et al., 2005).

In recent years, several geothermal wells have been drilled in the Gaoyang uplift, and their temperatures are the highest (about 116°C) in North China Plain (Wang et al., 2020b). The Gaoyang uplift has geothermal heating and cascading utilization potential (Wu et al., 2018). However, there is little research on the genetic mechanism of geotherms in the Gaoyang uplift. This article intends to discuss the genetic mechanism of the high geothermal anomaly in the Gaoyang uplift by using geophysical methods.

GEOLOGICAL CONDITION

Gaoyang uplift belongs to the third structural unit in the Jizhong depression (class II) of the North China Basin (class I), which is located in the south central part of the Jizhong depression (**Figure 1**). The Gaoyang uplift is adjacent to the Lixian slope, with Baoding sag in the west, Raoyang sag in the east, Niutuozhen uplift and Baxian sag in the north and northeast, and Wuji-Gaocheng uplift and Jinxian sag in the southwest. The buried hill roof is deeply buried, and the main body is between 2.8 and 4 km, with a region of about 70 km^2.

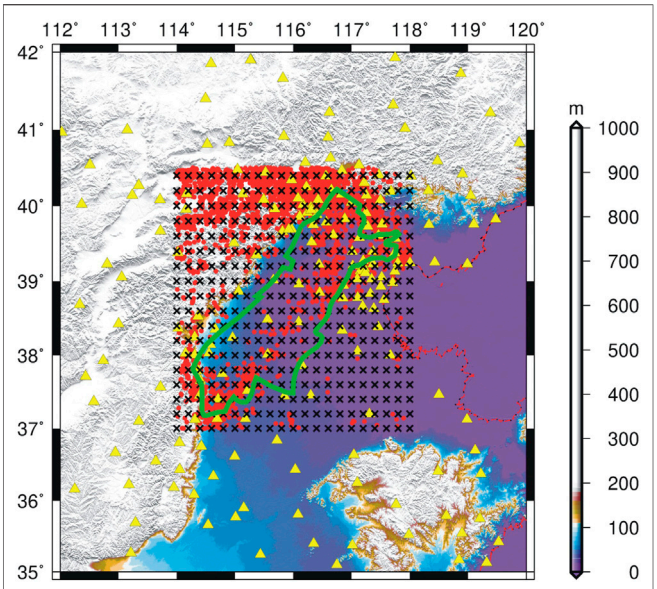

FIGURE 2 | Seismic events (red dots) and stations (yellow triangles). Grid points of 0.2° (black oblique cross) and the green frame (Jizhong depression).

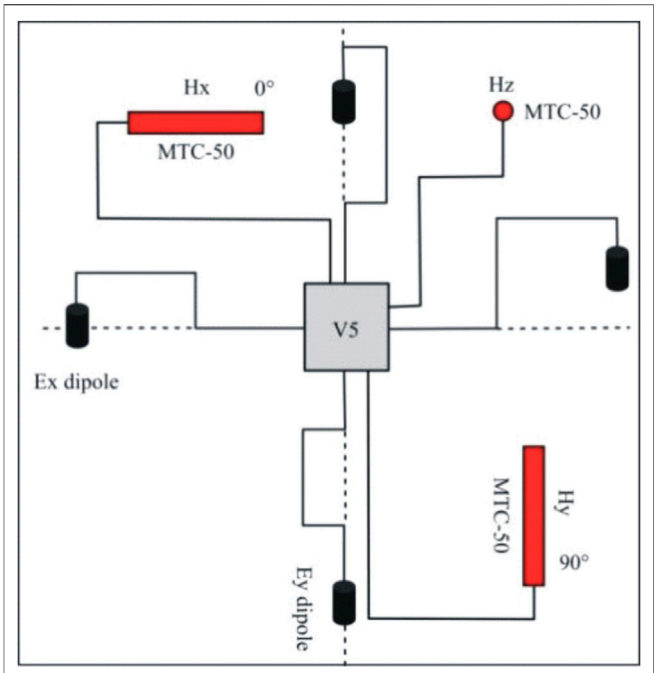

FIGURE 3 | Diagram of the MT station layout in the Jizhong depression.

The karst thermal reservoir dominated by marine carbonate rocks of the Proterozoic Wumishan formation is thick and widely distributed (Ye, 1983).

The Yanshan movement is the most important tectonic movement in this area, and a series of NE, NWW, and EW trending inherited tensile faults have been developed. The Taihang Mountain in the west and the Yanshan Mountain in the northwest are uplifted, and the Jizhong depression subsides as a whole. However, the interior of the Jizhong depression is uneven and distributed in the NE-SW direction, accompanied by a large number of secondary faults and folds (Yan et al., 2000).

Near NE trending faults such as the Gaoyangdong fault, the Anguo fault and other small faults mainly grew in the main part of the Gaoyang uplift. The Gaoyangdong fault is a group of reverse-slope normal faults with strikes similar to that of NE that form the boundary between the Gaoyang uplift and Lixian slope (Jin et al., 2017). Regionally, the Gaoyang uplift is distributed in the NE direction. The strata of the Paleogene and Jixian systems are in angular unconformity contact, forming an unconformity surface. Deep faults and unconformities are channels for fluid migration. The main thermal reservoir of the Gaoyang uplift is dolomite of the Wumishan formation, and the caprock is sandstone and mudstone of the Quaternary, Neogene, and Paleogene.

From the early to later stages, the strata of the Gaoyang uplift include Archean (Ar), Changcheng system (Ch), and Jixian system (Jx) of Middle and Lower Proterozoic; Cambrian-Ordovician (Є-O) of Lower Paleozoic, Jurassic-Cretaceous (J-K) of Mesozoic; and Paleogene (E), Neogene (N), and Quaternary (Q) of Cenozoic. The buried hill carbonate strata are mostly made of Wumishan, as well as some Cambrian and Ordovician formations. The caprocks of thermal reservoirs are generally sandstone and mudstone of the Paleogene, Neogene, and Quaternary. The Paleogene is in angular unconformity contact with Jixian, Cambrian, or Ordovician strata.

GEOPHYSICAL METHODS

P-wave velocity imaging and magnetotelluric sounding were used for this study.

P-Wave Velocity Imaging

The data for P-wave velocity imaging were natural seismic events recorded by fixed observation stations during 2008 and 2019 in the study area and its adjacent area. Seismic events occurring in 114–118°E and 37–40.5°N with travel time residual≤0.5 S and seismic stations located in 112–120°E and 35–42°N were selected for the study. In order to obtain the pair of seismic data, we selected the control parameters of seismic phase data. The controlling parameters were set as follows. Firstly, the number of pairs for each earthquake is no more than 20 earthquakes. Secondly, the distance from the earthquake to the station is no more than 600 km. Thirdly, the distance between each pair of earthquakes is between 1 and 10 km. Finally, the number of seismic phases required for each pair is between 8 and 50. After screening, there are 6,036 seismic events and 90,980 primaries of P-wave from 193 stations used (**Figure 2**).

The initial velocity model of one dimension, which was established through multiple inversion tests based on the inversion results of the velocity structure in North China (Yu et al., 2010; Duan et al., 2016), was used.

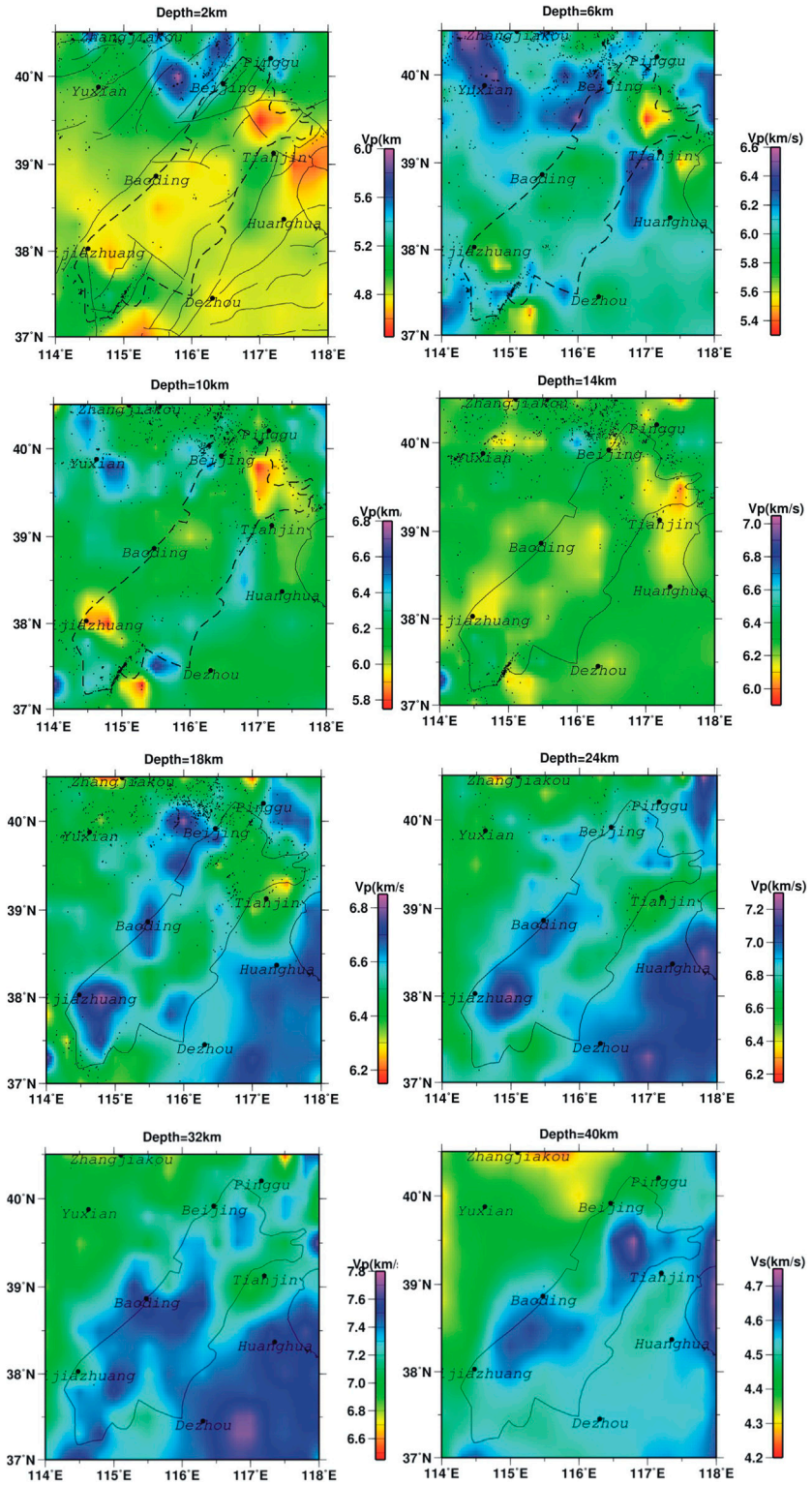

FIGURE 4 | P-wave velocity imaging at different depths in the Jizhong depression and its surroundings.

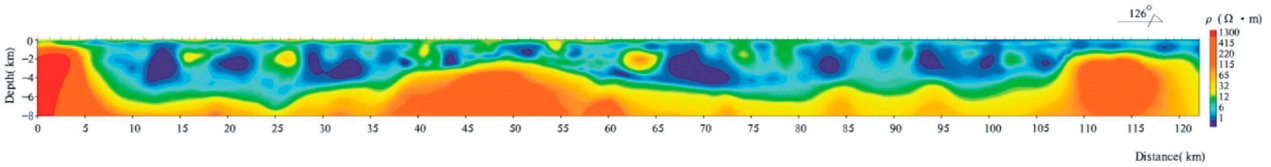

FIGURE 5 | 2D magnetotelluric inversion map.

Magnetotelluric Sounding

One section named MT01 was arranged for magnetotelluric sounding (**Figure 1**), with an average dot pitch of 1 km and a length of about 122 km. It crosses multiple geological structural units (Zhang et al., 2008), and a total of 122 points were recorded. In order to ensure the length of the apparent resistivity and impedance phase, the recording time of all measuring points that were collected at night was more than 12 h. Besides, reference stations are arranged to eliminate relevant noise.

A networked multifunctional electrical instrument, named V5, developed by Phoenix Geophysical Corporation of Canada, was selected for this study. The instrument contains a portable and solid acquisition system and a GPS synchronization system by which all recording units are synchronized within ±0.2 microseconds. The frequency range of the system is 10,000~0.000005 Hz. The frequency range of this study was 10,000~0.001 Hz in order to obtain information from depths of 6,000 to 10,000 m. Besides, the tensor observation method was adopted (**Figure 3**).

We used the imaging software system (MTSoft2d 2.4) with functions of two-dimensional magnetotelluric processing and inversion interpretation to preprocess data such as decoding and conversion, data editing, smoothing, polarization mode discrimination, and static correction. The preprocessed data were first inversed for one-dimensional inversion by using the method named Occam. The result was taken as the initial model to carry out two-dimensional nonlinear conjugate gradient (NLCG) to obtain the two-dimensional profile of magnetotelluric inversion.

GEOPHYSICAL RESULTS

P-Wave Velocity Imaging

Based on the velocity results of the seismic sounding profile in the working area (Duan et al., 2016), the initial velocity model was comprehensively constructed, for which the grid space in the horizontal dimension was $0.2^{\circ} \times 0.2^{\circ}$ and the depth of the grid in the vertical dimension was 0, 2, 6, 10, 14, 18, 24, 32, and 40 km. The P-wave of crust in the study area was fitted by using the Heda method.

In general, the travel time residuals of P-waves are distributed in the range of -1–1s after inversion. The P-wave velocity imaging maps of 2, 6, 10, 14, 18, 24, 32, and 40 km in the vertical dimension were obtained (**Figure 4**). It can be seen that the velocity of P-wave has an obvious lateral difference at the same depth, and the velocity of P-wave increases and then decreases with the increase of depth.

Magnetotelluric Sounding

The result of the magnetotelluric profile (**Figure 5**) shows that it is non-homogeneous for electrical structure in the Jizhong depression, and there are three layers for electrical structure in the longitudinal direction. The surface layer shows low resistance with high frequency, which is inferred to be the Quaternary incompact layer. The middle layer is characterized by low resistance (lower than the surface resistance) with medium frequency, which is inferred to be the interbedding of Neogene and Paleogene sandstone and mudstone. The deep layer is characterized by high resistance with medium and low frequency, which is inferred to be Mesozoic or Paleozoic limestone or carbonate rock. In the horizontal direction, it shows that the terrain of high resistance with medium and low frequency is undulating. High resistance buried shallow is the convex area, while high resistance buried deep is the concave area.

ANALYSIS AND DISCUSSION

Regional Crustal Thickness

According to the slice of P-wave velocity imaging at 2 km depth, the P-wave velocity decreased significantly after entering the North China Plain from the uplift of the Taihang Mountain. In the area where Paleozoic strata and Precambrian bedrock are widely exposed in the Taihang Mountain, it shows a high-speed anomaly. While in the Jizhong depression, which is located in the North China Plain, it shows a P-wave velocity anomaly that is consistent with the previous research results (Li et al., 2006; Qi et al., 2006; Lei et al., 2008).

As the depth increases to 20 km, the high-speed and low-speed anomalies are distributed alternately, and the corresponding relationship with the surface tectonic unit weakens. The velocity in the Jizhong depression still presents a low-speed anomaly, but the velocity value increases.

At a depth of 40 km, the change of P-wave velocity is as high as 6%, taking the Taihang piedmont fault as the boundary. The Taihang Mountain located in the west of the Taihang fault shows a low-speed anomaly (Wang et al., 2003), while the Jizhong

TABLE 1 | Resistivity of regional formation.

Number	Age	Resistivity (Ω·m)
1	Q	20
2	N, E	3–9
3	O, Є	200–300
4	J_{xw}	1,000

TABLE 2 | Geologic framework of JZ04.

Number	Depth(m)	Age	Lithology
1	0–455	Q	Mud, sand
2	455–1950	N	Mudstone, sandstone
3	1950–3,070	E	Mudstone, sandstone
4	3,070	J_{xw}	Dolomite

depression located in the east shows high-speed anomaly. The low-velocity anomaly at the depth of the Taihang Mountain may be caused by the upwelling, intrusion, or crustal warming of thermal materials in the upper mantle. Moreover, the heterogeneity of material composition in the crust–mantle transition zone is also a factor causing the heterogeneity of velocity.

The depth fluctuation of the Moho surface is inversely related to the fluctuation of the Cenozoic sedimentary basement. In the Jizhong depression located east of the Taihang piedmont fault, the buried depth of the Moho surface is relatively shallow, and it is mantled at a depth of 40 km. According to the deep reflection data of artificial seismic, the depth of the Moho surface in the Jizhong depression is about 32 km, which gradually deepens westward into the Taihang Mountain, and the maximum depth is about 42 km in the Taihang Mountain (Duan et al., 2016).

Tectonic Fracture

According to P-wave velocity imaging at different depths, there is an obvious velocity difference between the Taihang uplift and Jizhong depression in the North China Plain because of the sedimentary layers. The Taihang piedmont fault is the boundary of the Jizhong depression, which has a tendency toward the northeast. Because of its influence, P-wave velocity below the sedimentary layer in the Jizhong depression is still a low-speed anomaly. As the depth increases, the low-speed anomaly range expands to the southeast. When the depth reaches 18 km, the speed of the low-speed abnormity increases a bit. We can conclude that the speed at 18 km is not affected by the Taihang piedmont fault. Therefore, it can be inferred that the cutting depth of the Taihang piedmont fault is about 18 km, which does not reach the Moho surface and does not belong to a deep fault (Xu et al., 2001; Yang et al., 2002; Xu et al., 2010). Wang Chunyong (Wang et al., 1994) also concluded that the Taihang piedmont fault is not a deep fault by analyzing the deep seismic reflection profiles cutting through different sections of the fault. He considered it to be a shovel slip fault with a steep upper and a slow lower.

The Northeast P-wave low-velocity anomaly appears at a depth of 14 km in the Jizhong depression. As the depth increases, the region of P-wave low-velocity anomaly expands all the way down to 32 km. It is considered to be caused by the reduction of formation wave velocity by a series of faults. The faults at that location are the Niudong fault and the Gaoyangdong fault. We conclude that the Niudong fault and the Gaoyangdong fault are deep faults. It is generally believed that the Niudong fault controls the Niutuozhen uplift, while the Gaoyangdong fault controls the Gaoyang uplift. The main activity period of the faults is later than the secondary fault of the depression (Zhou et al., 2010).

Due to the dislocation of the strata on both sides caused by the fault, the fracture zone is generated, which makes the fault appear as a banded resistivity anomaly zone on the resistivity profile. Based on this, we identified the Taihang piedmont fault, Gaoyang west fault, Gaoyang east fault, Suning fault, Hejian fault, and so on according to the two-dimensional inversion profile of magnetotelluric resistivity. But small- and medium-sized faults in the Cenozoic caprock could not be identified because of the large distance between points measured by the magnetotelluric method. The multi-stage and multi-level spatial inherited faults of tectonic activities and the karst fissures in the Wumishan formation of the Jixian system are channels for thermal convection of deep fluids.

Stratigraphic Strata and Basement Undulation

According to the electrical characteristics of magnetotelluric sounding, the variation of low-high or low-high-low-high in the profile corresponds to the difference in electrical values of different lithologic strata, and the dense spacing of resistivity isolines shows the lithologic interface. After studying the logging data of 7 oil wells in the Jizhong depression (Shi et al., 2018), the resistivity of the regional formation was obtained (**Table 1**). It can be seen that among the sedimentary strata in the Jizhong depression, the resistivity of the Proterozoic Jixian system is the highest, followed by the Ordovician, Cambrian, and Qingbaikou systems, and the resistivities of the Neogene and Paleogene are the lowest. It should be noted that the resistivity obtained is the direct current resistivity, which is different from the magnetotelluric resistivity. However, the relative resistivity of different formations does not change. **Table 1** can still be used to explain the magnetotelluric profile in this study.

In the magnetotelluric profile, the Proterozoic Jixian system is the highest resistivity layer that belongs to the regional marker bed. The lithology of JZ04 is as follows (**Table 2**). The geological interpretation of the profile in the Jizhong depression (**Figure 6**) is compiled and combined with the JZ04 borehole. The profile is divided into 6 structural units, including the Taihang piedmont plain, Baoding sag, Gaoyang uplift, Lixian slope, Baxian sag, and Cangxian bulge. This forms a concave-convex structural pattern. The Gaoyang uplift belongs to low uplift, which is controlled by the Gaoyangdong fault. The buried depth of high resistivity carbonate rock at the section is 2,800~3300 m. Baoding sag

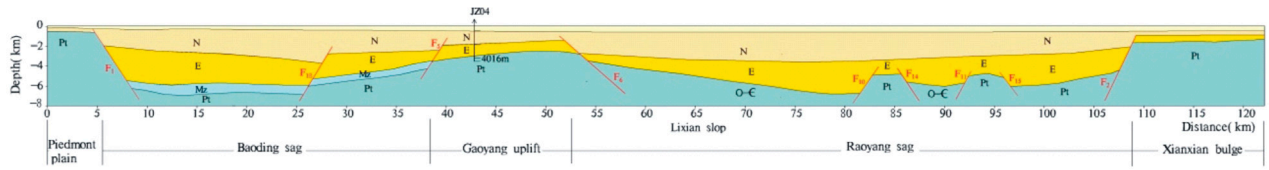

FIGURE 6 | Geological interpretation of MT.

is located in the west of the Gaoyang uplift, which is controlled by the Gaoyang fault. The buried depth of high resistivity in the sag is about 6 km. The east of the Gaoyang uplift is the Lixian slope, whose high resistivity is more than 4 km. To the east is Raoyang sag, whose depth of high resistivity is 4~6.5 km.

ANALYSIS OF THE HEAT SOURCE MECHANISM

The terrestrial heat flow of a sedimentary basin is made up of two parts (Birch et al., 1968). One part is crustal heat flow, whose heat comes from the decay of radioactive elements such as U, Th, and K in the shallow crust. The other part is the mantle heat flow, which comes from the deep mantle. Qiu Nansheng (Qiu et al., 2000) believes that the mantle heat flow accounts for more than 60% of the earth's heat flow according to the calculation of 10 km of sedimentary caprock in the North China Basin. As the Gaoyang uplift is located at the secondary unit of the Jizhong depression in the North China basin, so the deep mantle heat flow is the main heat source.

The North China Craton resulted in a massive thinning of the lithosphere. Seismic tomography results show that the thickness of the crust in the Jizhong depression is about 32 km. The thinner crust thickness reduces the distance for deep fluid to convert into the shallow crust, and that provides good conditions for deep heat energy to enter the shallow crust (Wang et al., 2017).

In recent years, helium derived from mantle was found in geothermal wells that indicated the invasion of materials from the mantle along the fault zone (Yang et al., 2018). Furthermore, the regional radon in the soil near the Xiadian fault is abnormally high (Miao et al., 2020), indicating the deep convection of fluid in the fault. According to the measurement of isotope gas geotemperature in the Niutuozhen geothermal field, the deep temperature of the Wumishan reservoir in the Jixian system is between 141 and 165°C. The contribution of helium derived from the mantle to the total helium content is 5~8%, indicating that the deep fault is a regional thermal control structure along which deep fluids are convecting into shallow reservoirs (Pang et al., 2018). The results of seismic tomography show that the cutting depth of the Gaoyangdong fault controlling the Gaoyang uplift reaches 28 km. The Gaoyangdong fault, which belongs to the tensile fault, is a deep fault. As an important channel, the fluid convection brings the deep heat flow to the shallow due to the difference in thermal potential.

There are sags on either side of the Gaoyang uplift. It forms a pattern of concave-convex structure which is conducive to the distribution and redistribution of heat flow in the Gaoyang uplift (Xiong and Gao, 1982). The pattern results in the formation temperature at the same depth being higher than that on both sides.

In addition, the thermal conductivity of Cenozoic sand and mudstone in the Gaoyang uplift is less than that of deep Jixian carbonate. Its thickness is more than 3000 m. The extremely thick caprock plays a good role in thermal insulation, which is the basic condition for the deep Jixian thermal reservoir to maintain a high temperature.

CONCLUSIONS

In this study, P-wave tomography and magnetotelluric sounding were used to probe the mechanism of high temperature in Gaoyang uplift, and the following conclusions were drawn:

1) The thickness of the crust in the Jizhong depression, where the Gaoyang uplift is located, is about 32 km. Compared with the Taihang Mountain uplift and Yanshan tectonic belt, the thickness of the crust is thinner, facilitating the heat flow of mantle into the shallow crust.
2) Each side of the Gaoyang uplift are sags. The concave-convex structure of the carbonate rock basement is convenient for heat flow to collect in the uplift area.
3) The thickness of Cenozoic sandstone and mudstone caprock in the Gaoyang uplift is about 3 km, which plays a good role in thermal insulation.
4) The cutting depth of the Gaoyang East fault is about 28 km, which is a large fault and provides a channel for convection of heat flow from the mantle to enter the shallow crust.

Comprehensive analysis shows that the crustal thickness in the Jizhong depression reducing, the tectonic pattern with concave and convex intersections, and the thickness of Cenozoic cap are the important conditions for the formation of regional geotherms. Compared with other uplifts in the Jizhong depression, the most important condition for high-temperature anomaly of heat storage in the Gaoyang uplift is that the Gaoyang East fault is a regional large fault, which provides conditions for deep geothermal fluid entering the shallow crust. Therefore, geothermal exploitation and utilization should be focused on the vicinity of the Gaoyang East fault and its intersecting faults in the future.

DATA AVAILABILITY STATEMENT

The raw data supporting the conclusions of this article will be made available by the authors without undue reservation.

AUTHOR CONTRIBUTIONS

QM studied the two methods and wrote the paper, GW provided suggestions for the structure of the paper, SQ studied the geology of the profile, LX studied the drill of JZ04, HX studied the P-wave velocity, and XZ studied the regional geology.

FUNDING

This study was financially supported by the grants from the geothermal survey project of the China Geological Survey (Grant No. DD20190555).

REFERENCES

Birch, F., Roy, R. F., and Decker, E. R., (1968). *Heat Flow and Thermal History in New York and New England: Studies of Appala Chian Geology: Northern and Maritime*. Editors E. Zen, W. S. White, J. B. Hadley, and J. B. Thopson (New York: Interscience), 437–451.

Cermark, V., and Rybach, L. (1989). Vertical Distribution of Heat Production in the Continental Crust. *Tectonophysic* 159, 217–230.

Chapman, D. S., and Rybach, L. (1985). Heat Flow Anomalies and Their Interpretations. *J. Geodyn.* 4 (1), 3–37. doi:10.1016/0264-3707(85)90049-3

Chen, M. X., and Deng, X. (1990). The Map of Geothermal Gradient of Cenozoic Sedimentary Cover in the North China Plain and its Brief Explanation. *Sci. Geol. Sin.* 3, 270–277. (in Chinese with English abstract).

Duan, Y., Wang, F., Zhang, X., Lin, J., Liu, Z., Liu, B., et al. (2016). Three dimensional Crustal Velocity Structure Model of the Middle-Eastern North China Craton (HBCrust1.0). *Sci. China Earth Sci.* 59, 1477–1488. doi:10.1007/s11430-016-5301-0

Gao, Z. J., Wu, L. J., and Cao, H. (2009). The Summarization of Geothermal Resources and its Exploitation and Utilization in Shandong Province. *J. Shandong Univ. Sci. Technology-Natural Sci.* 28 (2), 1–7. (in Chinese with English abstract). doi:10.16452/j.cnki.sdkjzk.2009.02.006

Jaupart, C., Labrosse, S., Lucazeau, F., and Mareschal, J.-C. (2015). Temperatures, Heat, and Energy in the Mantle of the Earth. *Earth Syst. Environ. Sci.* 7, 223–270. doi:10.1016/b978-0-444-53802-4.00126-3

Jin, F. M., Cui, Z. Q., Wang, Q., Li, L., Ren, C. L., Cui, M. Y., et al. (2017). Distribution Characteristics and Main Controlling Factors of Stratigraphic-Lithologic Reservoirs in Jizhong Depression. *Lithol. Reserv.* 29 (2), 19–27. doi:10.3969/j.issn.1673.8926.2017.02.003

Lei, J. S., Xie, F. R., Lan, C. X., Xing, C. Q., and Ma, S. Z. (2008). Seismic Images under the Beijing Region Inferred from P and P_mP Data. *Phys. Earth Planet Interi* 168 (3-4), 134–146. doi:10.1016/j.pepi.2008.06.005

Li, Z. W., Xu, Y., Hao, T. Y., Liu, J. S., and Zhang, L. (2006). Seismic Tomography and Velocity Structure in the Crust and Upper Mantle Around Bohai Sea Area. *Chin. J. Geophys.* 49 (3), 797–804. (in Chinese). doi:10.1002/cjg2.884

Lin, W. J., Chen, X. Y., Gan, H. N., and Yue, G. F. (2020). Geothermal, Geological Characteristics and Exploration Direction of Hot Dry Rocks in the Xiamen Bay-Zhangzhou Basin, Southeastern China. *Acta Geol. Sin.* 94 (7), 2066–2077. doi:10.19762/j.cnki.dizhixuebao.2020223

Miao, Q. Z., Wang, G. L., Xing, L. X., Zhang, W., Zhou, X. N., and Wang, W. Q. (2020). Study on Application of Deep Thermal Reservoir by Using Geophysical and Geochemical Methods in the Jizhong Depression Zone. *Acta Geol. Sin.* 94 (7), 2147–2156. doi:10.19762/j.cnki.dizhixuebao.2020225

Oskooi, B., Pedersen, L. B., Smirnov, M., Árnasonb, K., and Manzellac, A.the DGP Working Group (2005). The Deep Geothermal Structure of the Mid-Atlantic Ridge Deduced from MT Data in SW Iceland. *Phys. Earth Planet. Inter.* 150 (1-3), 183–195. doi:10.1016/j.pepi.2004.08.027

Pang, J. M., Pang, Z. H., and Lu, M. (2018). Geochemical and Isotopic Characteristics of Fluids in the Niutuozhen Geothermal Field, North China. *Environ. Earth Sci.* 77 (1), 1–12. doi:10.1007/s12665-017-7171-y

Qi, C., Zhao, D. P., Chen, Y., Chen, Q. F., and Wang, B. S. (2006). 3-D P and S Wave Velocity Structures and Their Relationship to Strong Earthquakes in the Chinese Capital Region. *Chin. J. Geophys.* 49 (3), 805–815. (in Chinese). doi:10.3321/j.issn:0001-5733.2006.03.024

Qiu, N. S. (2000). Discussion on Genesis Models of Thermal Evolution in Different Sedimentary Basins. *Petroleum Explor. Dev.* 27 (2), 15–17. doi:10.3321/j.issn:1000-0747.2000.02.005

Shi, Z., Zhang, H., and Duan, T. (2018). Investigation of Oil and Gas Reservoir in Jizhong Depression Based on Time-Frequency Electromagnetic Method. *Glob. Geol.* 37 (02), 585–594. (in Chinese with English abstract). doi:10.3969/j.issn.1004-5589.2018.02.025

Turcote, D. L., and Schubert, G. (1982). *Geodynamics: Application of Continuum Physics to Geological Problems*. New York: John Wiley and Sons.

Urzua, L., Powell, T., Cumming, W. B., and Dobson, P. (2002). *Apacheta, A New Geothermal Prospect in Northern Chile*, 26. US: Transactions-Geothermal Resources Council.

Villas, R. N., and Norton, D. (1977). Irreversible Mass Transfer between Circulating Hydrothermal Fluids and the Mayflower Stock. *Econ. Geol.* 72 (8), 1471–1504. doi:10.2113/gsecongeo.72.8.1471

Wang, C. Y., Zhang, X. K., Wu, Q. J., and Zhu, Z. P. (1994). Seismic Evidence of Detachment in North China Basin. *Chin. J. Geophys.* 37 (5), 613–620. (in Chinese).

Wang, G. L., Gao, J., Zhang, B. J., Xing, Y. F., Zhang, W., and Ma, F. (2020b). Study on the Thermal Storage Characteristics of the Wumishan Formation and Huge Capacity Geothermal Well Parameters in the Gaoyang Low Uplift Area of Xiong'an New Area. *Acta Geol. Sin.* 94 (7), 1970–1980. doi:10.19762/j.cnki.dizhixuebao.2020235

Wang, G. L., Liu, Y. G., and Zhu, X. (2020a). The Status and Development Trend of Geothermal Resources in China. *Earth Sci. Front.* 27 (1), 001–009. doi:10.13745/j.esf.2020.1.1

Wang, G. L., Zhang, W., Liang, J. Y., Lin, W. J., Liu, Z. M., and Wang, W. L. (2017b). Evaluation of Geothermal Resources Potential in China. *Acta Geol. Sin.* 38 (4), 449–459. doi:10.3975/cagsb.2017.04.02

Wang, G. L., Zhang, W., Lin, W. J., Liu, F., Zhu, X., Liu, Y. G., et al. (2017a). Research on Formation Mode and Development Potential of Geothermal Resources in Beijing-Tianjin-Hebei Region. *Geol. China* 44 (6), 1074–1085. (in Chinese with English abstract). doi:10.12029/gc20170603

Wang, S. Y., Xu, Z. H., and Pei, S. P. (2003). Velocity Structure of Upper Most Mantle beneath North China from P_n Tomography and its Implications. *Sci. China Ser. D Earth Sci.* 33 (2), 130–140. doi:10.1002/cjg2.431

Wang, Y., Wang, J. Y., Xiong, L. P., and Deng, J. F. (2001). Lithospheric Geothermics of Major Geotectonic Units in China Mainland. *Acta Geosci. Sin.* 22 (1), 17–22. (in Chinese with English abstract). doi:10.3321/j.issn:1006-3021.2001.01.004

Wu, A. M., Ma, F., Wang, G. L., Liu, J. X., Hu, Q. Y., and Miao, Q. Z. (2018). A Study of Deep-Seated Karst Geothermal Reservoir Exploration and Huge Capacity Geothermal Well Parameters in Xiong'an New Area. *Acta Geosci. Sin.* 39 (5), 523–532. (in Chinese with English abstract). doi:10.3975/cagsb.2018.071104

Xiong, L. P., and Gao, W. A. (1982). Characterics of Geotherm in Uplift and Depression. *Chin. J. Geophys.* 25 (5), 60–68. (in Chinese with English abstract).

Xu, J., Gao, Z. W., Sun, J. B., and Song, C. Q. (2001). A Preliminary Study of the Coupling Relationship between Basin and Mountain in Extensional Environments. *Acta Geol. Sin.* 75 (2), 165–174. doi:10.3321/j.issn:0001-5717.2001.02.004

Xu, M.-C., Gao, J.-H., Rong, L.-X., Wang, G.-K., and Wang, X.-J. (2010). Seismic Analysis of the Active Character of the Taihang Mountain Piedmont Fault. *Appl. Geophys.* 7 (4), 392–398. doi:10.1007/s11770-010-0265-x

Yan, D. S., and Yu, Y. T. (2000). *Evaluation and Utilization of Geothermal Resources in Beijing-Tianjin-Hebei Oil Region*. (Beijing: China University of Geosciences Press), 8–95. (in Chinese).

Yang, M. H., Liu, C. Y., Yang, B. Y., and Zhao, H. G. (2002). Extensional Structures of the Paleogene in the Central Hebei Basin,China. *Geol. Rev.* 48 (1), 58–67. doi:10.16509/j.georeview.2002.01.011

Yang, Q. Y., Wu, Q. J., Sheng, Y. R., Gao, J. Y., Song, J., and Di, L. (2018). Regional Seismic Body Wave Tomography and Deep Seismogenic Environment beneath Zhangbo Seismic Belt and its Adjacent Area. *Chin. J. Geophys.* 33 (8), 3251–3262. (in Chinese with English abstract). doi:10.6038/cjg2018L0628

Ye, L. J. (1983). *North China Platform Sedimentary Formation*. Beijing: Science Press. (in Chinese).

Yu, X. W., Chen, Y. T., and Zhang, H. (2010). Three-dimensional Crustal P-Wave Velocity Structure and Seismicity Analysis in Beijing-Tianjin-Tangshan Region. *Chin. J. Geophys.* 53 (8), 1817–1828. (in Chinese). doi:10.3969/j.issn.0001-5733.2010.08.007

Zhang, W. C., Yang, X. D., Chen, Y. J., Qian, Z., Zhang, C. W., and Liu, H. F. (2008). Sedimentary Structural Characteristics and Hydrocarbon Distributed Rules of Jizhong Depression. *Acta Geol. Sin.* 82 (8), 1103–1112. (in Chinese with English abstract). doi:10.16509/j.georeview.2002.01.011

Zhou, C. A., Li, X. P., Xin, W. J., Li, H. L., Wu, G. Q., Wu, X. L., et al. (2010). Research on Hydrocarbon Accumulating Conditions of Internal Buried Hills Exploration in Niutuozhen Uplift in Jizhong Sag. *China Pet. Explor.* 2010 (2), 29–32. doi:10.3321/j.issn:0001-5717.2008.08.011

Conflict of Interest: The authors declare that the research was conducted in the absence of any commercial or financial relationships that could be construed as a potential conflict of interest.